

Model-Free Predictive Control: Introductory Algebraic Calculations, and a Comparison with HEOL and ANNs

Cédric Join^{1,†} Emmanuel Delaleau^{**} Michel Fliess^{***,****,†}

* CRAN (CNRS, UMR 7039), Université de Lorraine, BP 239, 54506 Vandœuvre-lès-Nancy, France (e-mail: cedric.join@univ-lorraine.fr)

** ENI Brest, UMR CNRS 6027, IRDL, 29200 Brest, France (e-mail: emmanuel.delaleau@eni.fr)

*** LIX (CNRS, UMR 7161), École polytechnique, 91128 Palaiseau, France (e-mail: michel.fliess@polytechnique.edu)

**** LJLL (CNRS, UMR 7238), Sorbonne Université, 75005 Paris, France (e-mail: michel.fliess@sorbonne-universite.fr)

† A.L.I.E.N., 7 rue Maurice Barrès, 54330 Vézelize, France (e-mail: {michel.fliess,cedric.join}@alien-sas.com)

Joint IFAC Conference: SSSC, TDS, COSY

Abstract: Model predictive control (MPC) is a popular control engineering practice, but requires a sound knowledge of the model. Model-free predictive control (MFPC), a burning issue today, also related to reinforcement learning (RL) in AI, is reformulated here via a linear differential equation with constant coefficients, thanks to a new perspective on optimal control combined with recent advances in the field of model-free control (MFC). It is replacing Dynamic Programming, the Hamilton-Jacobi-Bellman equation, and Pontryagin's Maximum Principle. The computing burden is low. The implementation is straightforward. Two nonlinear examples, a chemical reactor and a two tank system, are illustrating our approach. A comparison with the HEOL setting, where some expertise of the process model is needed, shows only a slight superiority of the later. A recent identification of the two tank system via a complex ANN architecture might indicate that a full modeling and the corresponding machine learning mechanism are not always necessary neither in control, nor, more generally, in AI.

Keywords: Predictive control, optimal control, model-free control, machine-learning.

1. INTRODUCTION

Recent advances, with a strong algebraic flavor, in signal processing and time series analysis, have been applied to energy forecasting by Fliess et al. (2018) and Wang et al. (2025). Those forecasts are easier to implement than the current machine-learning approaches which are prominent now in AI. A similar goal is pursued here with *model-free predictive control (MFPC)*, which is a natural extension of *model-predictive control (MPC)*, one of the most popular control engineering practice, where the mathematical modeling should be well known (see, e.g., Rawlings et al. (2017)). Our approach to this hot topic (see, e.g., Khalilzadeh et al. (2021), Mesbah et al. (2022)) may be summarized as follows. We use the *ultra-local model of model-free control (MFC)* (Fliess and Join (2013, 2022)) like Belal Hossen and Habibullah (2025), Feng et al. (2024), He et al. (2023), Hegendus et al. (2023), Huo and Li (2025), Lammouchi et al. (2024), Li et al. (2025), Liu et al. (2024), Long et al. (2023), Mousavi et al. (2025), Rahmani et al. (2025), Sun et al. (2023a), Sun et al. (2023b), Sun et al. (2025), Xu et al. (2021), Xu et al. (2024), Wang and Wang (2020), Yang et al. (2025), Yin et al. (2024b), Yuan et al. (2024), Zhang et al. (2020a), Zhang et al. (2020b), Zhang et al. (2025a), Zhang et al. (2025b) Zhou et al. (2025), Zhou et al. (2022). A new understanding of optimal control (Join et al. (2024b, 2025)) via an algebraic interpretation of controllability (Fliess (1990), Fliess et al. (1995)) simplifies the connection between predictive and optimal controls. On a small time lapse, where a time-varying quantity may be approximated by a constant, the Euler-Lagrange equation, i.e., the fundamental equation of the calculus of variations (see, e.g., Gelfand and Fomin (1963)), becomes a constant linear ordinary differential equation. It leads to a dramatic simplification of the connection between predictive control and *reinforcement learning (RL)*, which is today a mainstay (see, e.g., Recht (2019), Adhau et al. (2024), Bertsekas (2024)). It vindicates the viewpoint expressed by LeCum (2024): *I do favor MPC over RL. I've been making that point since at least 2016. RL requires ridiculously large numbers of trials to learn any new task.*

If the key condition of a good model knowledge is not met, many studies use various artificial neural network (ANN) architectures to apply efficiently MPC techniques, without the need for MFPC. See, e.g., Åkesson and Toivonen (2006), Nubert et al. (2020), Ren et al. (2022), Salzmann et al. (2023), Adhau et al. (2024), and references therein. The same two tank example used by Adhau et al. (2024) via a *recurrent neural network* (see, e.g., Aggarwal (2018)) for its modeling is treated here with our ultra-local model of order 1 (Fliess and Join (2013)), and yields, therefore, a trivial implementation. Is this an indication that ANNs do not always provide the best solution? The other example studied is a chemical reactor (Pannochia and Rawlings (2003), Rawlings et al. (2017)), which was introduced in order to study the robustness of MPC with respect to disturbances. In those references, a time-invariant linearized modeling around a setpoint is used. It is therefore assumed that the reactor is always near the setpoint. This most stringent condition is lifted in our approach. In both cases, we are comparing our results with the *HEOL* approach (Join et al. (2024a)), already used by Delaleau et al. (2025), which is combining flatness-based and model-free controls. Although HEOL requires more process knowledge, its performance is not really superior.

Our paper is organized as follows. MFPC is introduced in Sect. 2 and HEOL in Sect. 3. Sect. 4.1 (resp. 4.2) depicts the chemical reactor (resp. the two tank system). See some concluding remarks in Sect. 5 and some reflections on modeling in AI. The mathematical modelings of the chemical reactor and of the two tank system are given in Appendices A and B for digital simulation purposes.

2. MODEL-FREE PREDICTIVE CONTROL

2.1 Ultra-local model

With Fliess and Join (2013) consider for simplicity's sake the SISO (single-input single output) *ultra-local model* or order 1, which is replacing the poorly known plant and disturbance description

$$\dot{y} = \mathcal{F} + \alpha u \tag{1}$$

The control and output variables are respectively u and y . The derivation order of y is 1 like in many concrete situations. \mathcal{F} subsumes not only the unknown structure of the system, which most of the time is nonlinear, but also any external disturbance. The constant $\alpha \in \mathbb{R}$ is chosen by the practitioner such that αu and \dot{y} are of the same magnitude. Therefore α does not need to be precisely estimated.

A data-driven estimation of \mathcal{F} in Eq. (1), which is obtained via algebraic manipulations (Fliess and Sira-Ramírez (2008b)), reads according to Fliess and Join (2013):

$$\mathcal{F}_{\text{est}}(t) = -\frac{6}{T^3} \int_0^T ((T - 2\sigma)y(t - T + \sigma) + \alpha(T - \sigma)\sigma u(t - T + \sigma)) d\sigma \tag{2}$$

Remark 2.1. Model-free control and the associated ultra-local model enjoy already many successes: See numerous references in Fliess and Join (2013, 2022), Join et al. (2024a), and, e.g., Ait Ziane et al. (2025), Michel et al. (2025) for sensor fault accommodation and an airfoil benchmark).

2.2 Optimization via the Euler-Lagrange equation

Preliminary calculations. Assume that $F = a$ is a constant in Eq. (1), which corresponds now to an elementary flat system, where y is a flat output. Introduce the Lagrangian, or cost function,

$$\mathcal{L} = (y - y_{\text{setpoint}})^2 + u^2 = (y - y_{\text{setpoint}})^2 + \left(\frac{\dot{y} - a}{\alpha}\right)^2$$

where y_{setpoint} denotes a given setpoint. For the criterion $J = \int_{t_i}^{t_f} \mathcal{L} dt$ the Euler-Lagrange equation (see, e.g., Gelfand and Fomin (1963)) $\frac{\partial \mathcal{L}}{\partial y} - \frac{d}{dt} \frac{\partial \mathcal{L}}{\partial \dot{y}} = 0$ corresponds to a non-homogeneous linear ordinary differential equation of 2nd order $\ddot{y} - \alpha^2(y - y_{\text{setpoint}}) = 0$. Any optimal solution reads $y^*(t) = y_{\text{setpoint}} + c_1 \exp(\alpha t) + c_2 \exp(-\alpha t)$, $c_1, c_2 \in \mathbb{R}$. It is independent of a ; c_1, c_2 are obtained via the two-point boundary conditions $y(t_i) = y_i$, $y(t_f) = y_{\text{setpoint}}$:

$$c_1 = \frac{y_i \exp(-\alpha t_f) - y_{\text{setpoint}} \exp(-\alpha t_f)}{\exp(\alpha t_i) \exp(-\alpha t_f) - \exp(-\alpha t_i) \exp(\alpha t_f)}$$

$$c_2 = -\frac{\exp(\alpha t_f)(y_i - y_{\text{setpoint}})}{\exp(\alpha t_i) \exp(-\alpha t_f) - \exp(-\alpha t_i) \exp(\alpha t_f)}$$

Application to MFPC. Consider the subdivision $0 < \dots < t_k < t_{k+1} < \dots < t_f$. On each time lapse $[t_k, t_{k+1}]$ replace \mathcal{F} in Eq. (1) by the constant $\mathcal{F}_{\text{est}}(t_k)$. Start the above optimization procedure again on the time horizon $[t_{k+1}, t_f]$. The criterion and the horizon may be modified if necessary.

3. THE HEOL SETTING

3.1 Tangent linear system

Differentiate \mathcal{A}_i in $\mathcal{A}_i(u_i, y_1, \dots, y_1^{(\nu_{i,1})}, y_2, \dots, y_2^{(\nu_{i,2})}) = 0$, $i = 1, 2$, where y_1, y_2 (resp. u_1, u_2) are *flat outputs* (resp. control variables) of a *flat system* (Fliess et al. (1995)):

$$\frac{\partial \mathcal{A}_i}{\partial u_i} du_i + \sum_{\iota=1,2} \frac{\partial \mathcal{A}_i}{\partial y_\iota} dy_\iota + \dots + \frac{\partial \mathcal{A}_i}{\partial y_\iota^{(\nu_\iota)}} dy_\iota^{(\nu_\iota)} = 0$$

where $dy_\iota^{(\mu_\iota)} = \frac{d^{\mu_\iota}}{dt^{\mu_\iota}} dy_\iota$. Associate to it the *tangent*, or *variational*, linear system, which is time-varying in general,

$$\frac{\partial \mathcal{A}_i}{\partial u_i} \Delta u_i + \sum_{\iota=1,2} \left(\frac{\partial \mathcal{A}_i}{\partial y_\iota} + \dots + \frac{\partial \mathcal{A}_i}{\partial y_\iota^{(\nu_\iota)}} \frac{d^{\nu_\iota}}{dt^{\nu_\iota}} \right) \Delta y_\iota = 0 \quad (3)$$

Δu_ι (resp. Δy_ι) is a control (resp. output) variable.

3.2 Homeostat

Assume that $\frac{\partial \mathcal{A}_i}{\partial y_\iota} \neq 0$, $\iota = 1, 2$, in Eq. (3). Then write with Join et al. (2024a) the *homeostat*

$$\frac{d}{dt}(\Delta y_\iota) = \mathfrak{F}_\iota + \alpha_\iota \Delta u_\iota, \quad \iota = 1, 2 \quad (4)$$

where

- $\alpha_\iota = -\frac{\frac{\partial \mathcal{A}_i}{\partial u_i}}{\frac{\partial \mathcal{A}_i}{\partial y_\iota}}$ is not constant in general;
- \mathfrak{F}_ι is not given by the missing terms in Eq. (3), but is data-driven, i.e., it corresponds to model mismatches and disturbances.

Write with Join et al. (2024a) the following estimate $\mathfrak{F}_{\iota, \text{est}}$, which is easily deduced from Eq. (2)

$$\mathfrak{F}_{\iota, \text{est}} = -\frac{6}{T^3} \int_0^T ((T-2\sigma)\Delta \tilde{y}_\iota(\sigma) + \sigma(T-\sigma)\tilde{\alpha}_\iota(\sigma)\Delta \tilde{u}_\iota(\sigma)) d\sigma \quad (5)$$

where

- the time lapse $T > 0$ is “small.”
- $\Delta \tilde{y}_\iota(\sigma) = \Delta y_\iota(\sigma + t - T)$, $\tilde{\alpha}_\iota(\sigma)\Delta \tilde{u}_\iota(\sigma) = \alpha_\iota(\sigma + t - T)\Delta u_\iota(\sigma + t - T)$.

3.3 *iP* controller

Mimicking Fliess and Join (2013), associate, with Join et al. (2024a), to the homeostat (4) the *intelligent proportional* (*iP*) controller

$$\Delta u_\iota = -\frac{\mathfrak{F}_{\iota, \text{est}} + K_{\iota, P} \Delta y_\iota}{\alpha_\iota}, \quad \iota = 1, 2 \quad (6)$$

where $K_{l,P} \in \mathbb{R}$ is the gain. Combine Eqs. (4) and (6): $(\frac{d}{dt} + K_{l,P}) \Delta y_l = 0$. Thus $\lim_{t \rightarrow \infty} \Delta y_l \approx 0$ if, and only if, $K_{l,P} > 0$.

4. COMPUTER EXPERIMENTS

4.1 Chemical reactor

Ultra-local model There are two control variables in the chemical reactor of Appendix A. We are therefore using twice Eq. (1). For the first (resp. second) case: $u = T_c$ (resp. $u = F$), $y = c$ (resp. $y = h$).

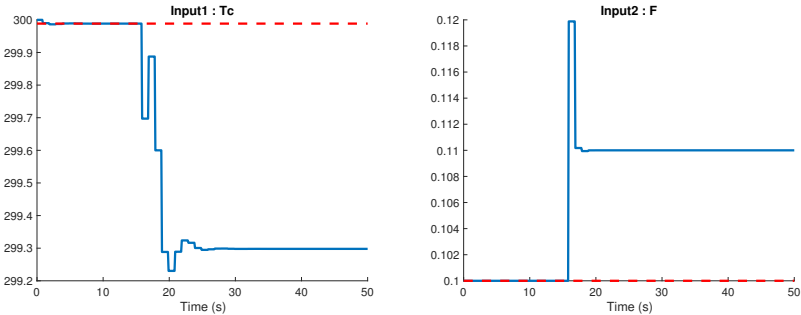
Homeostat for HEOL Eqs. (4) and (A.1) yield

$$\frac{d}{dt} \Delta c = \mathfrak{F}_c - \frac{2EUk_0 \exp(-\frac{E}{RT})c}{RC_p r \rho T^2} \Delta u_c$$

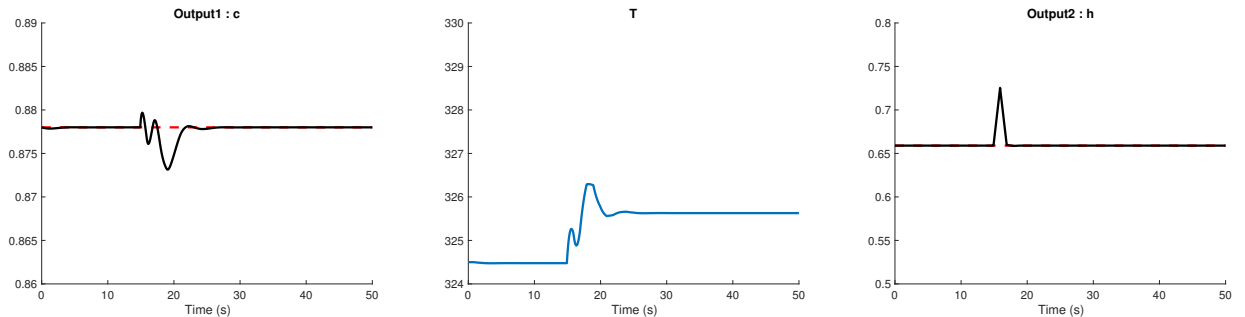
and

$$\frac{d}{dt} \Delta h = \mathfrak{F}_h - \frac{1}{\pi r^2} \Delta u_h$$

Simulations We follow Pannochia and Rawlings (2003) and Rawlings et al. (2017). For the initial operating point, $c(0) = 0.878 \text{ kmol/m}^3$, $T(0) = 324.5 \text{ K}$, $h(0) = 0.659 \text{ m}$, $T_c(0) = 300 \text{ K}$, $F(0) = 0.1 \text{ m}^3/\text{min}$. The sampling time for the control variables (resp. Eq. (2) and (5)) is 1 min (resp. 0.1 min). The total duration is 50 min. For MFPC, set for the first (resp. second) ultra-local model (1) $\alpha = -0.05$ (resp. $\alpha = -5$). According to Sect. 2.2, a new optimal trajectory is calculated every minute. For HEOL, set $K = 1$ for the gain in the iP (6). Reference trajectories are deduced from classic Bézier curves (see, *e.g.*, Rogers (2001)). Introduce the following disturbance: An unmeasured increase of the flow F of 10%. We seek to maintain the initial operating point for c and h : See Figs. 1 and 2. The figures above show a certain superiority of HEOL over MFPC. It should be added, however, that MFPC's results are satisfactory and, above all, do not require any knowledge of the model.



(a) T_c (– blue) and nominal control (– – red) (b) F (– blue) and nominal control (– – red)



(c) c (– black) and its reference trajectory (– – red)

(d) T

(e) h (– black) and its reference trajectory (– – red)

Fig. 1. Chemical reactor: HEOL

4.2 Two tank system

Ultra-local system Use Eq. (1), where, according to Appendix B, $y = h_2$.

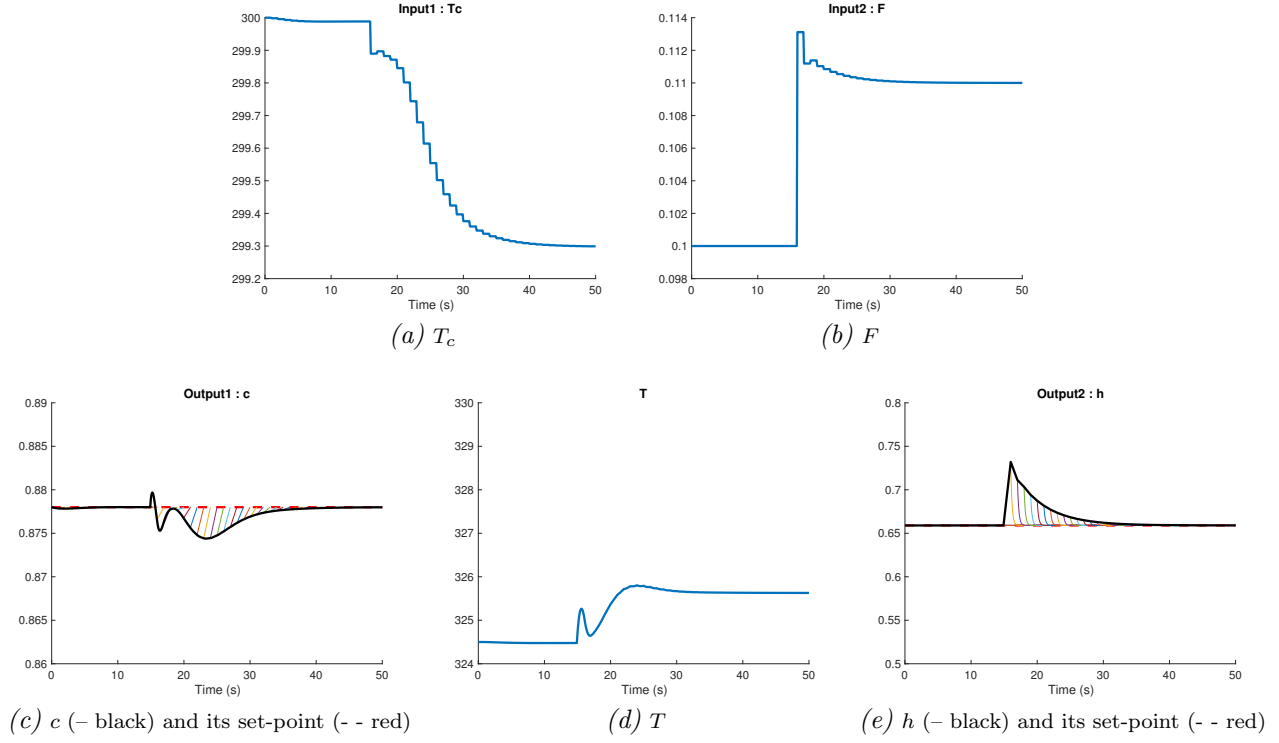


Fig. 2. Chemical reactor: MFPC

Homeostat Eq. (B.1) yields by differentiation:

$$d\dot{h}_2 = \frac{1}{s_2} \left(-\frac{k_2}{2\sqrt{h_2}} dh_2 - s_1 d\dot{h}_1 + du \right)$$

The corresponding homeostat reads :

$$\frac{d}{dt} \Delta h_2 = \mathfrak{F} + \frac{1}{s_2} \Delta u$$

Thus $\alpha = \frac{1}{s_2}$ is constant.

Simulations An additive white Gaussian noise $\mathcal{N}(0,0.1)$ corrupts the measurement. Simulations last 400s with a sampling period of 0.1s. For the iP controller associated to the homeostat command set $K = 0.1$. For the MFPC the time horizon is 2s. Our experiments mimic Adhau et al. (2024). Introduce an uncertainty $\nabla = 0.2$: The parameters are now $k_1(1 + \nabla)$ and $k_2(1 - \nabla)$. Without changing the control law parameters, the tracking remains excellent. As shown in Fig. 3, the control variable differs nevertheless from the nominal one. According to Fig. 4, the setpoints are well reached via the MFPC despite the uncertainty. Moreover the constraints in Appendix B on the control variable and the water levels are respected.

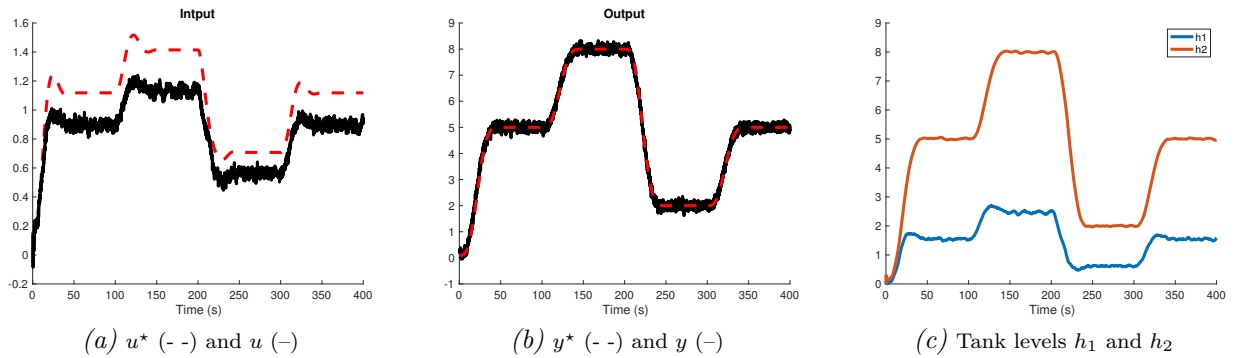
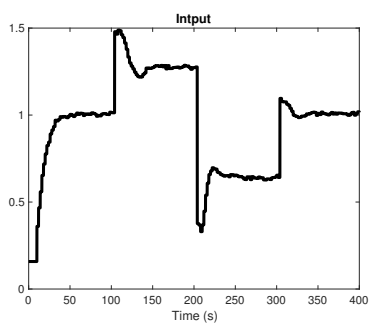
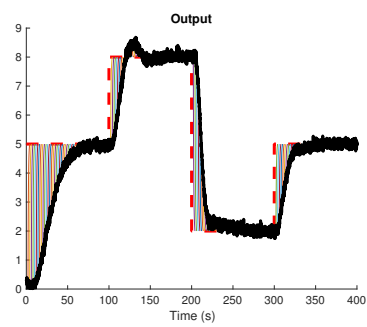


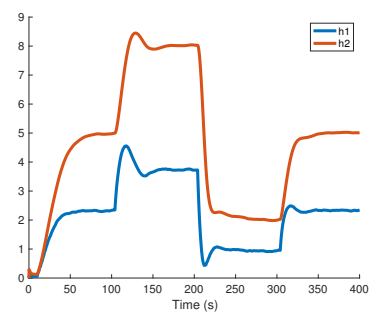
Fig. 3. Two tanks: HEOL



(a) $u (-)$



(b) Setpoint (- -) and $y (-)$



(c) Tank levels h_1 and h_2

Fig. 4. Two tanks: MFPC

5. CONCLUSION

Although the above simulations look encouraging, most important issues on constraints and stability are missing. Promising preliminary results will soon be presented.

The remarkable advances in modern AI often rely on models striving for comprehensiveness, along with their associated machine learning mechanisms. While outside the realm of control theory, the term *large language model (LLM)* exemplifies this trend towards comprehensive modeling, reflecting the significant energy resources required for their development (see, e.g., Xu and Poo (2023)). LeCun (2023) has said more than once about LLM and generative AI: *Machine learning sucks*. This skepticism is not alien to our techniques, which might be more subtle, at least in some parts of control engineering and robotics.

REFERENCES

- Adhau S., Gros S., Skogestad S. (2024). Reinforcement learning based MPC with neural dynamical models. *Europ. J. Control*, 80:101048.
- Aggarwal C.C. (2018). *Neural Networks and Deep Learning: A Textbook*. Springer, 2018.
- Ait Ziane M., Join C., Zasadzinski M. (2025). Sensor fault accommodation: a model-free framework. *Int. J. Contr.*, doi.org/10.1080/00207179.2025.2482182
- Åkesson B.M., Toivonen H.T. (2006) A neural network model predictive controller. *J. Process Contr.*, 16:937-946.
- Belal Hossen M., Habibullah M. (2025). Robust model-free predictive torque control for induction motor drive based on an ultralocal model. *IEEE Access*, 3550924
- Berbertsekas J. (2024). Model predictive control and reinforcement learning: A unified framework based on dynamic programming. *IFAC-PapersOnLine*, 58:363-383
- Delaleau E., Join C., Fliess M. (2025). Synchronization of Kuramoto oscillators via HEOL, and a discussion on AI. *IFAC PapersOnLine* **59-1**:229–234
- Feng Y., Zhang C., Huang S., Zhang S., Qu J., Li Z., Hue Z. (2024). An improved model-free predictive current control for PMSM drives based on current circle tracking under low-speed conditions. *IEEE Access*, 12:57767–57779.
- Fliess M. (1990). Some basic structural properties of generalized linear systems. *Syst. Contr. Lett.*, 15:391–396.
- Fliess M., Join C. (2013). Model-free control. *Int. J. Contr.*, 86:2228–2252.
- Fliess M., Join C. (2022). An alternative to proportional-integral and proportional-integral-derivative regulators: Intelligent proportional-derivative regulators. *Int. J. Robust Nonlin. Contr.*, 32:9512–9524.
- Fliess M., Join C., Sira-Ramírez H. (2008a). Non-linear estimation is easy *Int. J. Model. Ident. Contr.*, 4:12-27.
- Fliess M., Join C., Voyant C. (2018). Prediction bands for solar energy: New short-term time series forecasting techniques. *Solar Energ.*, 166:519-528.
- Fliess M., Lévine J., Martin P., Rouchon P. (1995). Flatness and defect of non-linear systems: introductory theory and examples. *Int. J. Contr.*, vol. 61:1327–1361.
- Fliess M., Sira-Ramírez H. (2008b). Closed-loop parametric identification for continuous-time linear systems via new algebraic techniques. H. Garnier, L. Wang (eds): *Identification of Continuous-time Models from Sampled Data*, pp. 362–391, Springer.
- Gelfand I.M., Fomin S.V. (1963). *Calculus of Variations* (translated from the Russian). Prentice-Hall.
- He D., Wang H., Tian Y., Christov N., Simeonov I. (2023). Trajectory tracking of two-stage anaerobic digestion process: A predictive control with guaranteed performance and saturated input, based on ultra-local model. *J. Process Contr.*, 129:103039.
- Hegedus T., Fenyés D., Van Tan V., Gaspar P. (2023). Lateral control for automated vehicles based on model predictive control and error-based ultra-local model. *Proc. 20th Internat. Conf. Informat. Contr. Automat. Robot.*, Rome.
- Huo X., Li P. (2025). Parameter-free ultralocal model-based predictive current control method for grid-tied inverters using extremum seeking control. *Contr. Engin. Pract.*, 157:106253.
- Join C., Delaleau E., Fliess M. (2024a). Flatness-based control revisited: The HEOL setting. *C.R. Math.*, 362:1693–1706.
- Join C., Delaleau E., Fliess M. (2024b). The Euler-Lagrange equation and optimal control: Preliminary results. *12th Internat. Conf. Syst. Contr.*, Batna, pp. 155–160, IEEEExplore.
- Join C., Delaleau E., Fliess M. (2025). Linear quadratic regulators: A new look. *Submitted*.
- Khalilzadeh M., Vaez-Zadeh S., Rodriguez J., Heydari R. (2021). Model-free predictive control of motor drives and power converters: A review. *IEEE Access* 9:105733-105747.
- Lammouchi Z., Labiod C., Srairi K., Benbouzid M., Khechekhouche A., Albalawi F., Ghoneim S.S.M., Ali E., Sharaf A.B.A. (2024). Experimental validation of model-free predictive control based on the active vector execution time for grid-connected system. *Sci. Rep.*, 14:30326.
- LeCun Y. (2023). X (*Twitter*), 22 December 2023.
- LeCun Y. (2024). X (*Twitter*), 25 August 2024.
- Li H., Lan D., Shao J., Tahir M. (2025) Model-free predictive current control of PMSM with online current gradient updating using ultra-local model. *IEEE Trans. Ener. Conver.*, doi: 10.1109/TEC.2025.3546661
- Liu X., Qiu L., Fang Y., Wang K., Li Y., Rodríguez J. (2024). A two-step event-triggered-based data-driven predictive control for power converters. *IEEE Trans. Indust. Electron.*, 719:13545–13555.
- Long B., Zhang J., Shen D., Rodríguez J., Guerrero J.M., Chong K.t. (2023). Ultralocal model-free predictive control of T-type grid-connected converters based on extended sliding-mode disturbance observer. *IEEE Trans. Power Electron.*, 38:15494–15508.
- Mesbah A., Wabersich K.P., Schoellig A.P., Zeilinger M.N., Lucia S., Badgwell T.A., Paulson J.A. (2022). Fusion of machine learning and MPC under uncertainty: What advances are on the horizon? *Amer. Contr. Conf.*, Atlanta, pp. 342-357.
- Michel L., Braud C., Barbot J.-P., Plestan F., Peaucelle D., Boucher X. (2025). Comparison of different feedback controllers on an airfoil benchmark. *Wind Energ. Sci.*, 10:177–191.
- Mousavi M.S., Nikmaram B., Nassaji A., Davari S.A., Flores-Bahamonde F., Rodríguez J. (2025). Applying model-free predictive current control with parallel cost functions for open-end winding synchronous reluctance motor. *IEEE Trans. Power Electron.*, 40:6801-6812.
- Nubert J., Köhler J., Berenz V., Allgöwer F., Trimpe S. (2020). Safe and fast tracking on a robot manipulator: Robust MPC and neural network control. *IEEE Robot. Automat. Lett.*, 5:3050-3057.

- Pannochia G., Rawlings J.B. (2003). Disturbance models for offset-free model-predictive control. *AIChE J.*, 49:426–439.
- Rahmani M., Davari S.A., Mousavi M.S., Zolfagharian R., Flores-Bahamonde F., Rodriguez J. (2025). Finite-set ultralocal model predictive current control with integral sliding mode observer for quadratic buck converters of data centers. *16th Power Electron. Drive Syst. Techno. Conf.*, Tabriz.
- Rawlings J.B., Mayne D.Q., Diehl M.M. (2017). *Model-Predictive Control: Theory, Computation, and Design* (2nd ed.). Nob Hill Publishing.
- Recht B. (2019). A tour of reinforcement learning: The view from continuous control. *Annual Rev. Contr. Robot. Auton. Syst.*, 2:253-279.
- Ren Y.M., Alhajeri M.S., Luo J., Chen S., Abdullah F., Wu Z., Christofides P.D.(2022). A tutorial review of neural network modeling approaches for model predictive control. *Comput. Chem. Engin.*, 165:107956.
- Rogers D.F. (2001). *An Introduction to NURBS with Historical Perspective*. Morgan Kaufmann.
- Salzmann T., Kaufmann E., Arrizabalaga J., Pavone M., Scaramuzza D., Ryll M. (2003). Real-time neural MPC: Deep learning model predictive control for quadrotors and agile robotic platforms. *IEEE Robot. Automat. Lett.*, 8: 2397-2404.
- Schoukens J., Noël J.-P. (2017). Nonlinear system identification: A user-oriented road map. *IFAC-PapersOnLine*, 5: 446-451.
- Sun Z., Deng Y., Wang J., H. Li H., Cao H. (2023a). Improved cascaded model-free predictive speed control for PMSM speed ripple minimization based on ultra-local model. *ISA Trans.*, 143:666–677.
- Sun Z., Deng Y., Wang J., Yang T., Wei Z., Cao H. (2023b). Finite control set model-free predictive current control of PMSM with two voltage vectors based on ultralocal model. *IEEE Trans. Power Electr.*, 38:776-788.
- Sun X., Huang Z., Yang Z., Lei G., T. Li T. (2025). Improved model-free predictive current control for suppressing inverter nonlinearity and parametric time-varying of PMSM drive systems. *IEEE Trans. Indus. Electron.*, doi: 10.1109/TIE.2025.3552258
- Xu L., Chen G., Li Q. (2021). Cascaded speed and current model of PMSM with ultra-local model-free predictive control. *IEEE Electr. Power Appl.*, 15:1424-1437.
- Xu B., Poo M. (2023). Large language models and brain-inspired general intelligence. *Natl. Sci. Rev.*, 10:267.
- Xu B., Wu Q., Ma J., Liu X., Fang Y. (2024). Improved non-cascaded continuous-set model-free predictive control scheme for PMSM drives. *IET Power Electron.*, <https://doi.org/10.1049/pe12.12830>
- Wang Z., Xu G., Sun R., Zhou A., Cook A., Chen Y. (2025). Online energy consumption forecast for battery electric buses using a learning-free algebraic method. *Sci. Rep.*, 15:1931.
- Wang Z., Wang J. (2020). Ultra-local model predictive control: A model-free approach and its application on automated vehicle trajectory tracking. *Contr. Engin. Pract.*, 181:104482.
- Yang A., Lu Z., Jiangchao Qin J. (2025). Ultra-local dual-torque model for model-free predictive torque control without weighting factors in induction motor drives. *Contr. Engin. Pract.*, 160:106327,
- Yin Z., Wang X., Su X., Shen Y., Xiao D., Zhao H. (2024b). A switched ultra-local model-free predictive controller for PMSMs. *IEEE Trans. Power Electron.*, 39:10665–10669.
- Yuan L., Mei J., Xu A., Li X. (2024). Model-free predictive control with super- twisting observer of single-phase neutral-clamped H-bridge cascade inverters with fixed switching frequency. *IEEE J. Emerg. Select. Topics Power Electron.*, 2024 doi: 10.1109/JESTPE.2024.3508749
- Zhang Y., Jiang T., Jiao J. (2020a). Model-free predictive current control of a DFIG using an ultra-local model for grid synchronization and power regulation. *IEEE Trans. Energy Convers.*, 35:2269–2280.
- Zhang Y., Liu X., Liu J., Rodriguez J., Garcia C. (2020b). Model-free predictive current control of power converters based on ultra-local model. *IEEE Internat. Conf. Indust. Techno.*, pp. 1089-1093, Buenos Aires.
- Zhang Z., Ma J., Qiu L., Liu X., Wu W., Fang Y. (2025a). Subspace predictor-based predictive voltage control for power converters. *IEEE Trans. Industr. Electron.*, doi: 10.1109/TIE.2025.3531479
- Zhang G., Yao X., Peretti L., Bai J., Gao X., Li Z. (2025b) Smooth nonlinear ESO-based model-free predictive current control with an extended control set for SPMSM drives. *IEEE J. Emerg. Select. Topics Power Electr.*, doi: 10.1109/JESTPE.2025.3528761
- Zhou Y., Liu T., Wang Y., Li H. (2025), Independent cost function model predictive current control for SMPMSM drive. *IEEE Trans. Industr. Electron.*, doi: 10.1109/TIE.2025.3555040
- Zhou Y., Wang Z., Zhou X., Shen H., Ahn J., Wang J. (2022). Extremum-seeking-based ultra-local model predictive control and its application to electric motor speed regulation. *IFAC-PapersOnLine*, 55-37:56-61.

Appendix A. A CHEMICAL REACTOR

Fig. A.1-(a) depicts a well-stirred chemical reactor, which was introduced by Pannochia and Rawlings (2003) and Rawlings et al. (2017) for investigating the robustness of linear time-invariant MPC with respect to disturbances. The following nonlinear model is used:

$$\begin{cases} \dot{c} = \frac{F_0(c_0 - c)}{\pi r^2 h} - k_0 \exp\left(-\frac{E}{RT}\right)c \\ \dot{T} = \frac{F_0(T_0 - T)}{\pi r^2 h} - \frac{\Delta H}{\rho C_p} k_0 \exp\left(-\frac{E}{RT}\right)c + \frac{2U}{r\rho C_p}(T_c - T) \\ \dot{h} = \frac{F_0 - F}{\pi r^2} \end{cases} \quad (\text{A.1})$$

where c (resp. h) is the fluid concentration (resp. height). Both quantities are measured. The control variables are F and T_c . In the computer experiments $F_0 = 0.1$, $T_0 = 350$, $c_0 = 1$, $r = 0.2149$, $k_0 = 7.2 \cdot 10^{10}$, $\frac{E}{R} = 8750$, $U = 54.94$, $\rho = 1000$, $C_p = 0.2149$, $\Delta H = -5 \cdot 10^4$.

Eq. (A.1) defines a *flat* system (Fliess et al. (1995)). It is straightforward to check that c and h are *flat outputs*:

$$F = -(\dot{h}\pi r^2 - F_0), \text{ and } T_c = \frac{(\dot{T} - F_0 \frac{T_0 - T}{\pi r^2 h} + \frac{\Delta H}{\rho C_p} k_0 \exp(-\frac{E}{RT})c)(r\rho C_p)}{2U} + T, \text{ where } T = \frac{-R}{E \log(\dot{c} + F_0 \frac{c_0 - c}{\pi r^2 h k_0 c})}.$$

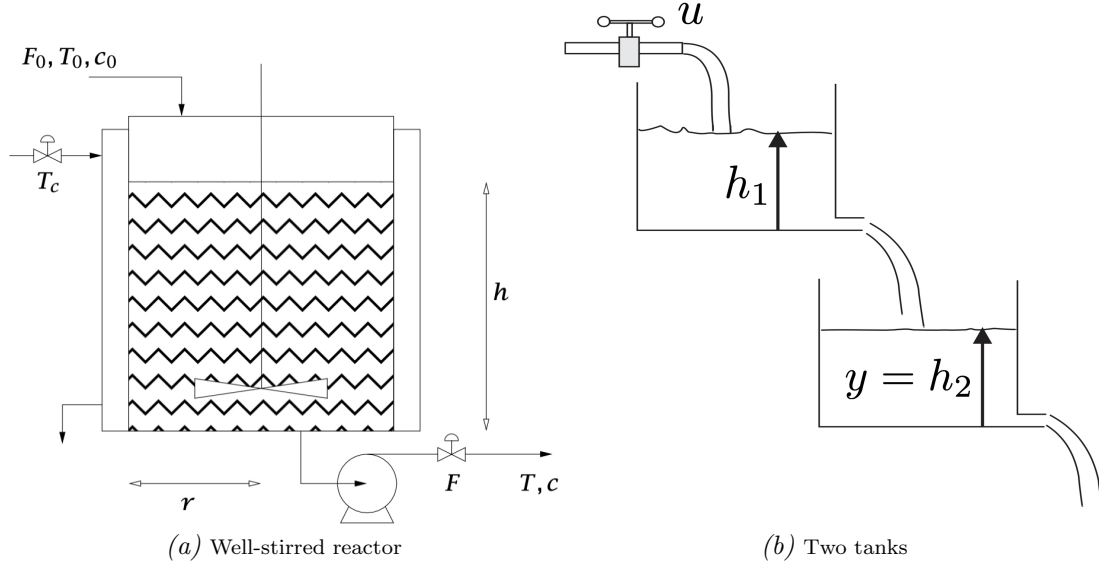


Fig. A.1. Process schemes

Appendix B. A TWO TANK SYSTEM

Consider with Adhau et al. (2024) the two tanks system described by Schoukens and Noël (2017):¹

$$\begin{cases} s_1 \dot{h}_1 = u - k_1 \sqrt{h_1} \\ s_2 \dot{h}_2 = k_1 \sqrt{h_1} - k_2 \sqrt{h_2} \end{cases} \quad (\text{B.1})$$

where $u \geq 0$ is the control variable, h_ι , $\iota = 1, 2$, $0 \leq h_\iota \leq 10$, is the water level, k_ι and s_ι are constant parameters. Eq. (B.1) defines a flat system, where h_2 is a flat output. In the computer experiments $s_1, s_2 = 1$, $k_1 = 0.6$, $k_2 = 0.5$.

¹ Fig. A.1-(b) is borrowed from Fliess et al. (2008a), where this system is examined via algebraic estimation techniques.